VNU Journal of Science: Mathematics - Physics

Journal homepage: https://js.vnu.edu.vn/MaP

Original Article

Unparticle Effects on Plasmon Production from Electron-positron Annihilation in SN 1987A

Ha Huy Bang[1], Truong Minh Anh[2,*]

[1]*VNU Hanoi University of Science, 334 Nguyen Trai, Thanh Xuan, Hanoi, Vietnam*

[2]*Faculty of Engineering Physics, Hanoi University of Science and Technology, 1 Dai Co Viet, Hanoi, Vietnam*

Received 24th December 2025
Revised 26th December 2025; Accepted 17th January 2026

Abstract: The unparticle effects on plasmon production at the $e^+ e^-$ collider in SN 1987A are investigated. We have calculated the energy loss and the cross-section of this process for different values of the scaling parameter d_U. By assuming the supernovae cooling rate $\dot{\varepsilon} \leq 7.288\times10^{-27}$ GeV, we find the lower bound on the scale Λ_U = 32.849 TeV, 11.655 TeV, 5.084 TeV, 2.770 TeV corresponding to d_U =1.6,1.7,1.8,1.9 and Λ_U = 0.675 TeV, 0.309 TeV, 0.168 TeV, 0.101 TeV corresponding to d_U = 2.1,2.2,2.3,2.4.

In addition, we have shown that in the range $\sqrt{s}$ =1 TeV – 13 TeV the cross-section varies from 4.663×10^{-20} barn to 6.206×10^{-3} barn. So, we hope that the cross-section gives possible experimental signatures for unparticle.

Keywords: Electron-positron annihilation, SN 1987A, energy loss rate, unparticle.

1. Introduction

In particle physics, unparticle physics [1] is a speculative theory that conjectures a form of matter that cannot be explained in terms of particle using the Standard Model, because its components are scale invariant. As we well know, in certain high-energy or astrophysical environments like supernovae or dense plasmas, photons can acquire an effective mass by interacting with the plasma, becoming what physicists call plasmon, which behave like massive photons.

* Corresponding author.
E-mail address: anh.truongminh@hust.edu.vn

https//doi.org/10.25073/2588-1124/vnumap.5101

In refs. [2-4], we have considered the effects of the unparticle on Bhabha scattering, on Axion-like particles production in e^+e^- collisions and plasmon plasmon scattering.

2. The Energy Loss Rate Per Unit Mass

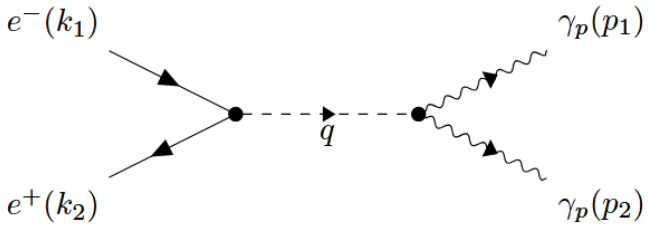

Figure 1. The Feynman diagram for $e^+e^- \longrightarrow \gamma_p\gamma_p$ process via unparticle.

The propagator of a scalar unparticle has the form

$$\frac{iA_{d_u}}{2\sin(d_u\pi)}\cdot(-q^2-i\varepsilon)^{d_u-2}, \tag{1}$$

here
$$A_{d_u}=\frac{16\pi^2\sqrt{\pi}\,\Gamma\left(d_u+\frac{1}{2}\right)}{(2\pi)^{2d_u}\Gamma(d_u-1)\Gamma(2d_u)}. \tag{2}$$

We need to note that the vertex of the electron-positron-scalar unparticle is given by [2, 5]

$$i\,\frac{\lambda_0}{\Lambda_u^{d_u-1}}\;-\;\frac{\lambda_1}{\Lambda_u^{d_u-1}}\,\gamma^5, \tag{3}$$

and the vertex of plasmon-plasmon-scalar unparticle is [5]

$$\frac{4i\lambda_3}{\Lambda_u^{d_u}}\left(-p_1\cdot p_2\cdot g^{\mu\nu}+p_1^{\nu}p_2^{\mu}\right). \tag{4}$$

From (1), (3), (4) we get the amplitude for the process as follows

$$iM=\bar{v}(k_2)\cdot\frac{(i\lambda_1-\lambda_2\gamma^5)}{\Lambda_u^{d_u-1}}\cdot\frac{iA_{d_u}}{2\sin(d_u\pi)}\cdot(-q^2-i\varepsilon)^{d_u-2}\cdot u(k_1)\cdot \times\frac{4i\lambda_3}{\Lambda_u^{d_u}}\cdot\left(-p_1\cdot p_2\cdot g^{\mu\nu}+p_1^{\nu}p_2^{\mu}\right)\cdot\varepsilon_{\mu}^{*}(p_1)\varepsilon_{\nu}^{*}(p_2). \tag{5}$$

Therefore, we obtain the total squared amplitude

$$|M|^2=\left|\bar{v}(k_2)(i\lambda_1-\lambda_2\gamma^5)u(k_1)\right|^2\frac{A_{d_u}^2}{4\sin^2(d_u\pi)}\frac{16\lambda_3^2}{\Lambda_u^{4d_u-2}}\cdot x\,q^{2(2d_u-4)}\cdot\left(-p_1\cdot p_2\cdot g^{\mu\nu}+p_1^{\nu}p_2^{\mu}\right)\left(-p_1\cdot p_2\cdot g^{\mu'\nu'}+p_1^{\nu'}p_2^{\mu'}\right)\mathrm{x}\,\varepsilon_{\mu}^{*}(p_1)\varepsilon_{\nu}^{*}(p_2)\varepsilon_{\mu'}(p_1)\varepsilon_{\nu'}(p_2). \tag{6}$$

By using $\sum_{i=1}^{3}\varepsilon_{\mu}^{*s}(p_1)\varepsilon_{\mu'}^{s}(p_1)=-g_{\mu\mu'}+\frac{p_{1\mu}p_{1\mu'}}{m_A^2}$, (7)

we have

$$|M|^2=\frac{16A_{d_u}^2\lambda_3^2}{\sin^2(d_u\pi)\,\Lambda_u^{4d_u-2}}|q^2|^{2d_u-4}\cdot[(\lambda_1^2-\lambda_2^2)(k_2\cdot k_1)-(\lambda_1^2+\lambda_2^2)m_e^2]\times\;[2(p_1\cdot p_2)^2+m_A^4]. \tag{8}$$

In the center of mass frame, four-momenta of particles are defined by

$$k_1=(E,\vec{p}),\quad k_2=(E,-\vec{p}),\quad p_1=\left(E,\overrightarrow{p'}\right),\quad p_2=\left(E,-\overrightarrow{p'}\right), \tag{9}$$

and $$s = q^2 = 4E^2 \ , \tag{10}$$

$$|\vec{p}| = \frac{\sqrt{s}}{2}\sqrt{1 - 4\frac{m_e^2}{s}}, \quad |\overrightarrow{p'}| = \frac{\sqrt{s}}{2}\sqrt{1 - 4\frac{m_A^2}{s}}. \tag{11}$$

From these, we obtain

$$|M|^2 = \frac{16A_{d_u}^2\lambda_3^2}{\sin^2(d_u\pi)\,\Lambda_u^{4d_u-2}} \cdot s^{2d_u-4}\left[(\lambda_1^2-\lambda_2^2)\frac{s}{2}\left(1-2\frac{m_e^2}{s}\right)-(\lambda_1^2+\lambda_2^2)m_e^2\right] \times\left[2\frac{s^2}{4}\left(1-2\frac{m_A^2}{s}\right)^2+m_A^4\right]. \tag{12}$$

The energy loss rate per unit mass of a supernovae at a temperature T is given by

$$\dot{\varepsilon} = \frac{T^4}{512\pi^5\rho_{SN}}\int_{m_e/T}^{\infty}dx_1\int_{m_e/T}^{\infty}dx_2\sqrt{x_1^2-\left(\frac{m_e}{T}\right)^2}\sqrt{x_2^2-\left(\frac{m_e}{T}\right)^2}\cdot\frac{1}{\left(e^{x_1-\frac{\mu_e}{T}}+1\right)}\frac{1}{\left(e^{x_2+\frac{\mu_e}{T}}+1\right)}\cdot \times\frac{e^{\frac{x_1+x_2-2\mu_A}{T}}}{\left(e^{\frac{x_1+x_2}{2}-\frac{\mu_A}{T}}-1\right)^2}\cdot|M|^2. \tag{13}$$

Introducing the dimensionless variables $x_i=E_i/T$ (i=1,2) and $E=(E_1+E_2)/2$, we can rewrite

$$\dot{\varepsilon} = \frac{T^{4d_U-2}\,\lambda_3^2A_{d_U}^2}{64\pi^5\rho_{SN}\sin^2(d_U\pi)\,\Lambda_u^{4d_U-2}}\int_{m_e/T}^{\infty}dx_1\int_{m_e/T}^{\infty}dx_2\sqrt{x_1^2-\left(\frac{m_e}{T}\right)^2} \times\sqrt{x_2^2-\left(\frac{m_e}{T}\right)^2}\frac{1}{\left(e^{x_1-\frac{\mu_e}{T}}+1\right)}\frac{1}{\left(e^{x_2+\frac{\mu_e}{T}}+1\right)}\cdot\frac{e^{x_1+x_2-2\mu_A/T}}{\left(e^{\frac{x_1+x_2}{2}-\frac{\mu_A}{T}}-1\right)^2} \times(x_1+x_2)^{4d_U-2}\left[\frac{T^4}{2}(x_1+x_2)^4\left(1-2\frac{m_A^2}{s}\right)^2+m_A^4\right]. \tag{14}$$

In Fig. 2, we have plotted the energy-loss rate $\dot{\varepsilon}$ as a function of the scale Λ_U for different values of d_U.

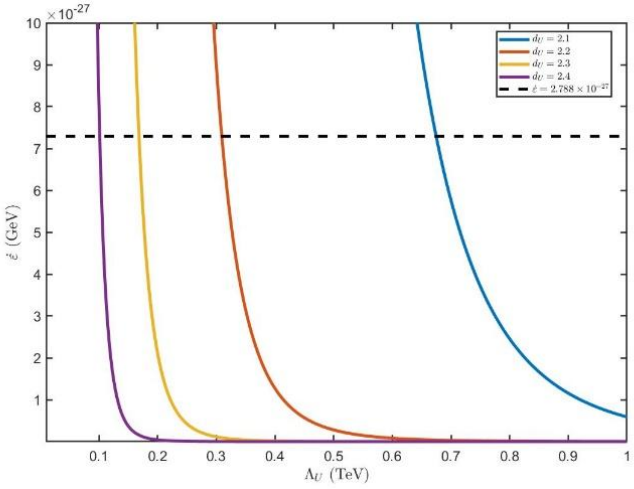

Figure 2. The energy-loss rate dε/dt is shown as a function of Λ_U. The upper horizontal line corresponds to the upper bound of the $\dot{\varepsilon}$ i.e. $\dot{\varepsilon} \lesssim 7.288\times10^{-27}$ GeV.

Below in Table 1 we have given the lower bound on Λ_U for different anomalous dimension d_U.

Table 1. The lower bound on Λ_U (follows from Fig. 2) corresponding to different d_U is shown

d_U	Λ_U (TeV)
1.6	32.849
1.7	11.655
1.8	5.084
1.9	2.770
2.1	0.675
2.2	0.309
2.3	0.168
2.4	0.101

In the past, the authors have found the lower bound on the Λ_U is in the range of 1 TeV to 10 TeV [6-8] and 1 TeV to 3 TeV [9]. Our results are consistent with the results in refs. [6-9] but more precise.

3. The Cross-section

From (12) we get the differential cross-section:

$$\frac{d\sigma}{d\Omega} = \frac{1}{16\pi^2}\frac{\sqrt{1-\frac{4m_A^2}{s}}}{\sqrt{1-\frac{4m_e^2}{s}}}\cdot\frac{A_{d_u}^2\lambda_3^2}{\sin^2(d_u\pi)\Lambda_u^{4d_u-2}}\cdot s^{2d_u-5}\left[(\lambda_1^2-\lambda_2^2)\frac{s}{2}\left(1-2\frac{m_e^2}{s}\right)-(\lambda_1^2+\lambda_2^2)m_e^2\right]$$
$$\times\left[2\frac{s^2}{4}\left(1-2\frac{m_A^2}{s}\right)^2+m_A^4\right]. \quad (15)$$

Therefore, the total cross-section is:

$$\sigma = \frac{A_{d_u}^2\lambda_3^2\cdot s^{2d_u-5}}{4\pi\sin^2(d_u\pi)\,\Lambda_u^{4d_u-2}}\frac{\sqrt{1-\frac{4m_A^2}{s}}}{\sqrt{1-\frac{4m_e^2}{s}}}\left[(\lambda_1^2-\lambda_2^2)\frac{s}{2}\left(1-\frac{2m_e^2}{s}\right)-(\lambda_1^2+\lambda_2^2)m_e^2\right]$$
$$\times\left[\frac{s^2}{2}\left(1-\frac{2m_A^2}{s}\right)^2+m_A^4\right]. \quad (16)$$

The cross-sections σ dependence on the $\sqrt{s}$ is shown in Fig. 3 for different values of d_U.

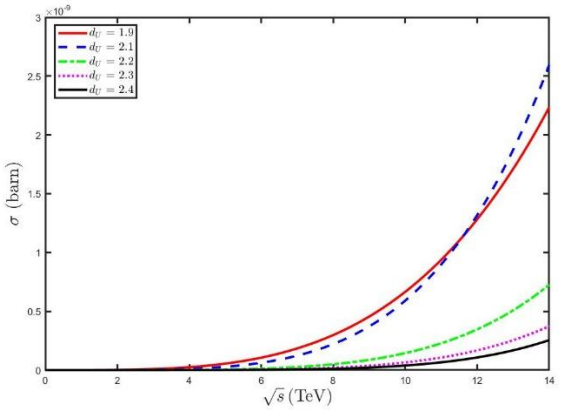

Figure 3. Total cross-section due to the unparticle contribution depending on the center of mass energy for du=1.9;2.1;2.2;2.3 and 2.4.

As we can observe from Fig. 3, the σ increases with $\sqrt{s}$.

We now turn to the numerical analysis. In tables 2 and 3, we provide our numerical results for the total cross section with: $\lambda_3 = \lambda_1 = 1$, $\lambda_2 = 1/\sqrt{2}$, $m_A = 19$ MeV, $m_e = 0.511$ MeV, $\sqrt{s}$ = 1 TeV−13 TeV. In table 2, d_U = 1.6,1.7,1.8,1.9 and in table 3, d_U = 2.1,2.2,2.3,2.4.

Table 2. The total cross-section of $e^+e^- \rightarrow \gamma_p\gamma_p$ process via unparticle exchange with $\lambda_3 = \lambda_1 = 1$, $\lambda_2 = 1/\sqrt{2}$, m_A =19 MeV, m_e = 0.511 MeV, $\sqrt{s}$ = 1 TeV−13 TeV and d_U =1.6,1.7,1.8,1.9.

$\sqrt{s}$ (TeV)	σ (barn)			
	d_U =1.6 Λ_U = 32.849 TeV	d_U =1.7 Λ_U = 11.655 TeV	d_U =1.8 Λ_U = 5.084 TeV	d_U =1.9 Λ_U = 2.770 TeV
1.0	4.663×10^{-20}	1.066×10^{-18}	2.429×10^{-17}	5.562×10^{-16}
2.0	2.461×10^{-19}	7.423×10^{-18}	2.233×10^{-16}	6.744×10^{-15}
3.0	6.513×10^{-19}	2.310×10^{-17}	8.171×10^{-16}	2.903×10^{-14}
4.0	1.299×10^{-18}	5.169×10^{-17}	2.052×10^{-15}	8.178×10^{-14}
5.0	2.219×10^{-18}	9.656×10^{-17}	4.190×10^{-15}	1.826×10^{-13}
6.0	3.438×10^{-18}	1.609×10^{-16}	7.509×10^{-15}	3.520×10^{-13}
7.0	4.977×10^{-18}	2.477×10^{-16}	1.230×10^{-14}	6.131×10^{-13}
8.0	6.857×10^{-18}	3.600×10^{-16}	1.885×10^{-14}	9.916×10^{-13}
9.0	9.096×10^{-18}	5.007×10^{-16}	2.748×10^{-14}	1.515×10^{-12}
10.0	1.171×10^{-17}	6.725×10^{-16}	3.850×10^{-14}	2.214×10^{-12}
11.0	1.472×10^{-17}	8.782×10^{-16}	5.223×10^{-14}	3.120×10^{-12}
12.0	1.814×10^{-17}	1.120×10^{-15}	6.900×10^{-14}	4.268×10^{-12}
13.0	2.199×10^{-17}	1.402×10^{-15}	8.915×10^{-14}	5.694×10^{-12}

Table 3. The total cross-section of $e^+e^- \rightarrow \gamma_p\gamma_p$ process via unparticle exchange with $\lambda_3 = \lambda_1 = 1$, $\lambda_2 = 1/\sqrt{2}$, m_A =19 MeV, m_e = 0.511 MeV, $\sqrt{s}$ = 1 TeV−13 TeV and d_U =2.1,2.2,2.3,2.4.

$\sqrt{s}$ (TeV)	σ (barn)			
	d_U =2.1 Λ_U = 0.675 TeV	d_U =2.2 Λ_U = 0.309 TeV	d_U =2.3 Λ_U = 0.168 TeV	d_U =2.4 Λ_U = 0.101 TeV
1.0	2.910×10^{-13}	6.723×10^{-12}	1.549×10^{-10}	3.587×10^{-09}
2.0	6.143×10^{-12}	1.873×10^{-10}	5.693×10^{-09}	1.740×10^{-07}
3.0	3.657×10^{-11}	1.312×10^{-09}	4.689×10^{-08}	1.685×10^{-06}
4.0	1.297×10^{-10}	5.218×10^{-09}	2.093×10^{-07}	8.438×10^{-06}
5.0	3.462×10^{-10}	1.523×10^{-08}	6.678×10^{-07}	2.944×10^{-05}
6.0	7.721×10^{-10}	3.654×10^{-08}	1.723×10^{-06}	8.173×10^{-05}
7.0	1.521×10^{-09}	7.657×10^{-08}	3.842×10^{-06}	1.938×10^{-04}
8.0	2.738×10^{-09}	1.454×10^{-07}	7.693×10^{-06}	4.093×10^{-04}
9.0	4.597×10^{-09}	2.558×10^{-07}	1.419×10^{-05}	7.915×10^{-04}
10.0	7.309×10^{-09}	4.242×10^{-07}	2.455×10^{-05}	1.428×10^{-03}
11.0	1.112×10^{-08}	6.703×10^{-07}	4.029×10^{-05}	2.435×10^{-03}
12.0	1.630×10^{-08}	1.018×10^{-06}	6.335×10^{-05}	3.964×10^{-03}
13.0	2.318×10^{-08}	1.495×10^{-06}	9.605×10^{-05}	6.206×10^{-03}

From numerical results, we have found that the cross-sections are about 10^{-20} barn − 10^{-12} barn with d_U = 1.6,1.7,1.8,1.9 and about 10^{-13} barn − 10^{-3} barn with d_U = 2.1,2.2,2.3,2.4. Therefore, the effects of unparticle on the cross-sections can be very strong. If the measurement is carried out at $\sqrt{s}$ = 1 TeV−13 TeV then the σ for the process $e^+e^- \rightarrow \gamma_p\gamma_p$ should be detectable.

4. Conclusions

It is well known that, constraints on dimensionless effective coupling constants (like g) are crucial in physics to test fundamental theories (Standard Model, beyond), search for new particles,... They act as powerful discriminators between models, using precision measurements from experiments. So, the results of our paper are useful for searching for unparticles. Furthermore, given the large cross section of the process in our paper, it is hoped that the signal of the unparticle can be detected.

References

[1] H. Georgi, Unparticle Physics, Phys. Rev. Lett., Vol. 98, 2007, pp. 221601.

[2] S. T. L. Anh, H. H. Bang et al., Unparticle Effects on Bhabha Scattering, Can. J. Phys., Vol. 96, No. 3, 2018, pp. 268.

[3] S. T. L. Anh, H. Huy Bang et al., Unparticle Effects on Axion-Like Particles Production in e^+e^- Collisions, Int. J. Theor. Phys., 2018, pp. 149.

[4] T. M. Anh, H. H. Bang, The Role of Radion in SN 1987A Cooling, Indian J. Phys., 2025, https//doi.org/10.1007/s12648-025-03848-x.

[5] H. F. Li, H. L. Li et al., Unparticle Effects on Top Quark Pair Production at Photon Collider, arXiv:0802.0236 [hep-ph].

[6] P. K. Das, Unparticle Effects in Supernovae Cooling, arXiv:0708.2812 [hep-ph].

[7] E. O. Iltan, The Annihilation Cross Section of the Dark Matter Which Is Driven by Scalar Unparticle, arXiv:1206.6988 [hep-ph].

[8] T. Kikuchi et al., Unparticle Physics at the Photon Collider**,** arXiv:0801.0018 [hep-ph].

[9] T. M. Aliev et al., Scalar Unparticle Signals at the LHC, arXiv:1701.00498 [hep-ph].